

Image Super-Resolution Reconstruction Based On Multi-Dictionary Learning

ShiMin¹, ZhuFeng¹, YI Qing-Ming¹

¹*School Of Information Science And Technology, Jinan University, Guangzhou, Guangdong 510632, China)*

ABSTRACT: In order to overcome the problems that the single dictionary cannot be adapted to variety types of images and the reconstruction quality couldn't meet the application, we propose a novel Multi-Dictionary Learning algorithm for feature classification. The algorithm uses the orientation information of the low resolution image to guide the image patches in the database to classify, and designs the classification dictionary which can effectively express the reconstructed image patches. Considering the nonlocal similarity of the image, we construct the combined nonlocal mean value(C-NLM) regularizer, and take the steering kernel regression(SKR) to formulate a local regularization ,and establish a unified reconstruction framework. Extensive experiments on single image validate that the proposed method, compared with several other state-of-the-art learning based algorithms, achieves improvement in image quality and provides more details.

Keywords: directional feature; multi-dictionary learning; combined nonlocal mean value(C-NLM); steering kernel regression(SKR)

I. INTRODUCTION

The aim of image super-resolution(SR) is to construct a high-resolution (HR) from one or more low-resolution (LR) images and additional information such as exemplar images or statistical priors using software techniques. Because it is easy to implement and it takes lower cost performance, the image super-resolution technique has been widely applied to surveillance, medical imaging,remote sensing, and so on. In recent years, the super-resolution algorithms based on sparse representation have become one of the hot issues in current research [1,2].Yang et al.[3,4] first introduced sparse coding theory to estimate high-frequency details from an over-complete dictionary. The approach performs well in recovering some high frequency information. But it often produces noticeable blurring artifacts along the edges.For the same assumption, Zeyde et al.[5] proposed a more efficient image super-resolution algorithm based on K-SVD dictionary learning.All of the above algorithms used a universal and over-complete dictionary to represent various image structures. However, sparse decomposition over a highly redundant dictionary is potentially unstable and tends to generate visual artifacts.To address the aforementioned problem in single dictionary, a large number of SR methods introduced the idea of classification to produce more compelling SR results.Yin et al.[6] proposed a sparse representation of texture constraints, which divides the image into different texture regions, and trains multiple texture dictionaries.Dong et al.[7] proposed an image super-resolution method combining sparse coding and regularized learning models into a unified SR framework. The methods can recover many high-frequency details, but it has the high computation complexity and slow convergence.

In this paper, the whole training set is divided into groups so that the patches in each group are similar in appearance and they are considered to locate in the same subspace. But How to divide these subspaces efficiently? The usual approach to apply the K-means algorithm to cluster image patches in database without exploiting the structural information from the low resolution itself. To address the aforementioned problems, we

propose a novel SR method based on Multi-Dictionary Learning algorithm for feature classification. Firstly, we adopt the curvelet transform to estimate the sixteen direction feature image in which all patches are clustered in several groups. Then each patch satisfying a certain condition in the database is classified into one of these groups with supervision of the clustering results, and Principal Component Analysis (PCA) is used to learn corresponding compact dictionaries for different groups by which we can obtain more accurate representation of subspaces of these patches. Moreover, considering spatial and directional information of patches, we construct the combined nonlocal mean value(C-NLM) regularization term, which is very helpful in preserving edge sharpness.

Single Image SR Model

So far, a variety of models have been proposed for SR recovery, and the most widely used observation model relating \mathbf{X} and \mathbf{Y} can be generally expressed as

$$\mathbf{Y} = \mathbf{S}\mathbf{H}\mathbf{X} + \nu \quad (1)$$

Where \mathbf{X} and \mathbf{Y} are the HR and LR images, respectively, \mathbf{S} and \mathbf{H} denote a down-sampling operator and a blurring filter respectively, and ν represents Gaussian noise. From the observation model, we know that the low quality observation image \mathbf{Y} is typically generated by blurring, down-sampling and noising. However, the objective of SR reconstruction is to solve the inverse problem of estimating the underlying HR image \mathbf{X} from the LR image \mathbf{Y} . That is to solve the following least squares problem:

$$\hat{\mathbf{X}} = \arg \min_{\mathbf{X}} \|\mathbf{Y} - \mathbf{S}\mathbf{H}\mathbf{X}\|_2^2 + \lambda E(\mathbf{X}) \quad (2)$$

Where $E(\mathbf{X})$ represents the regularization term constructed from a prior knowledge, and λ is a regularization parameter. To obtain the additional information of image, this paper integrates the HR reconstruction term, local and non-local regularization terms, and example-based hallucination term into the unified SR framework like Eq. (2). Mathematically, it is defined as

$$\hat{\mathbf{X}} = \arg \min_{\mathbf{X}} \left\{ \begin{array}{l} \|\mathbf{Y} - \mathbf{S}\mathbf{H}\mathbf{X}\|_2^2 + \lambda_1 E_{sparse}(\mathbf{X}) \\ + \lambda_2 E_{nonlocal}(\mathbf{X}) + \lambda_3 E_{local}(\mathbf{X}) \end{array} \right\} \quad (3)$$

Where $\|\mathbf{Y} - \mathbf{S}\mathbf{H}\mathbf{X}\|_2^2$ is the reconstruction term to ensure that the reconstructed HR image should be consistent with the LR input via back-projection. The second term $E_{sparse}(\mathbf{X})$ is the sparse hallucination regularization term, which requires that the estimated HR image has a sparse representation over a multi-dictionary learnt from the LR itself and the database image. The third term $E_{nonlocal}(\mathbf{X})$ is the non-local prior that assumes that each HR pixel can be predicted by weighting average of a large neighborhood. The last local prior regularization term indicates that each HR pixel should be perfectly estimated from a small local area around it.

Feature classification dictionary-based hallucination

2.1 Curvelet-Based Direction Extraction

Curvelet transform is an efficient representation for preserving edges since it has very high directional sensitivity and is highly anisotropic [8]. Therefore, in this paper, we apply the curvelet transform to extract directional features which are then used for classified dictionary learning and weight estimation. Considering different sizes of \mathbf{X} and \mathbf{Y} , we firstly apply bicubic interpolation to magnify \mathbf{Y} to obtain the initial estimate of the high resolution image \mathbf{X}^0 , which is the same size as \mathbf{X} . Then the curvelet coefficients of the image \mathbf{X}^0 can be obtained by $\mathbf{Q}=\Gamma(\mathbf{X}^0)$. where Γ represents the curvelet transform matrix. \mathbf{Q} is a set of curvelet coefficients expressed as $\{\mathbf{Q}_{c,l} | c=1,\dots,C;l=1,\dots,L_c\}$, in which C and L_c are the total number of scales and directions at the c th scale, respectively.

Because of the directional symmetry, we partition the curvelet coefficient matrices at the finest scale into 16 direction subsets, denoted as $\{\mathbf{F}_f\}_{f=1}^{16}$. The directional features of the initial estimate image in 16 different directions can be defined as

$$\mathbf{A}_f = |\Gamma^{-1}(\mathbf{H}_f(\mathbf{Q}))| \quad (4)$$

Where Γ^{-1} stands for the inverse curvelet transform, and $\mathbf{H}_f(\mathbf{Q}) = \begin{cases} \mathbf{Q}_{c,l}, & \text{if } \mathbf{Q}_{c,l} \in \mathbf{F}_f \\ 0, & \text{otherwise} \end{cases}$.

Obviously, The directional feature image $\mathbf{A}_f (f = 1, \dots, 16)$ can be obtained by Eq.(4).

2.2 Learning Classification Dictionary

To make full use of the additional information of LR images, we propose a multi-dictionary learning algorithm based on directional feature classification. First, We adopt the K-means algorithm to partition \mathbf{A}_f obtained in Section 2.1 into K clusters $\mathbf{C}_k = \{\mathbf{s}_i^k, i=1,\dots,m; k=1,\dots,K\}$, where k and i denote Category number and sample patch number respectively. K and m represent the total number of Category and the total number of sample patch, then obtain $\boldsymbol{\mu}_k (k=1,\dots,K)$ the centroid of cluster \mathbf{C}_k and the radius $\mathbf{r}_k = \max \|\mathbf{s}_i^k - \boldsymbol{\mu}_k\|_2, i=1,\dots,m$. To construct a more effective dictionary, we use the high-pass filter to extract high-frequency information from high-resolution image of database as the feature. Then we obtain a set of high-frequency patches \mathbf{X}_G . Let $\mathbf{x}_{G_i} (i=1,\dots,g)$ be an image patch in the \mathbf{X}_G and compute the distance (d_i^k) between \mathbf{x}_{G_i} and $\boldsymbol{\mu}_k$. An image patch \mathbf{x}_{G_i} will be added to the \mathbf{C}_{k_i} th class if the minimum value of d_i^k , denoted by $d_i^{k_i}$, is smaller than threshold $\xi \mathbf{r}_{k_i}$ in which ξ is a constant to weight the similarity between the patches of database and the center of the centroid of cluster. Suppose that $\mathbf{C}_k = \{\mathbf{s}_i^k, i=1,\dots,M; k=1,\dots,K\}$ is the K clusters after augmentation, where M is the total number of sample patch. Apply the PCA to all of the

K subdatasets, we could get K subdictionaries $\mathbf{D}_k (k=1, \dots, K)$.

2.3 Reconstruction with sparse representation

Our method is based on the sparse representation of image patches which demonstrates effectiveness and robustness in regularizing super-resolution problem. Suppose that $\mathbf{X} \in \mathbb{R}^N$ and $\hat{\mathbf{X}} \in \mathbb{R}^N$ represent the HR and reconstructed HR images, respectively. Suppose that $\mathbf{x}_i \in \mathbb{R}^n$ and $\hat{\mathbf{x}}_i \in \mathbb{R}^n, i=1, \dots, p$ represent the HR and the reconstructed HR image patches, and here, p is the number of image patches. The image patches are overlapped with each other in our method to reduce blocking artifacts. An HR image patch can be written as $\mathbf{x}_i = \mathbf{R}_i \mathbf{X}$, and here, $\mathbf{R}_i \in \mathbb{R}^{n \times N}$ represents the extracting matrix. In previous sections, we have learnt the K subdictionaries \mathbf{D}_k . Recall that we have the centroid $\boldsymbol{\mu}_k$ of each cluster available, and hence we could select the best fitted subdictionary to $\hat{\mathbf{x}}_i$ by calculating the minimum distance between $\hat{\mathbf{x}}_i$ and $\boldsymbol{\mu}_k$, i.e. $k_i = \arg \min_k \|\mathbf{x}_i - \boldsymbol{\mu}_k\|_2^2$. Then the k_i th subdictionary \mathbf{D}_{k_i} will be selected and assigned to patch $\hat{\mathbf{x}}_i$. The sparse representation of $\hat{\mathbf{x}}_i$ over the subdictionary \mathbf{D}_{k_i} is given as: $\hat{\mathbf{x}}_i \approx \mathbf{D}_{k_i} \boldsymbol{\alpha}_i, s.t. \|\boldsymbol{\alpha}_i\|_0 \leq T, i=1, \dots, p$. where $\boldsymbol{\alpha}_i$ is the sparse representation coefficient, T is a scalar controlling the sparsity[9]. The updated HR image \mathbf{Z} can be reconstructed by merging all the constructed patches and averaging the overlapping regions between the adjacent patches[10], i.e.,

$$\hat{\mathbf{Z}} = \left(\sum_{i=1}^p \mathbf{R}_i^T \mathbf{R}_i \right)^{-1} \sum_{i=1}^p \mathbf{R}_i^T \mathbf{D}_{k_i} \boldsymbol{\alpha}_i \quad (5)$$

Construct the regularization terms and SR recovery

3.1 Sparse hallucination regularization term

The sparse hallucination regularization term enforces the constrain that the reconstructed HR image $\hat{\mathbf{X}}$ should perfectly be consistent with by a multi-dictionary learnt from the LR input itself and the database, i.e., $\|\hat{\mathbf{X}} - \mathbf{Z}\|_2^2 \leq \varepsilon^2$. We formulate the sparse hallucination regularization term as:

$$E_{sparse}(\mathbf{X}) = \|\hat{\mathbf{X}} - \mathbf{Z}\|_2^2 \quad (6)$$

3.2 Combined non-local mean regularization term

Considering that there are often many repetitive patterns throughout a natural image. Such nonlocal redundancy is very helpful to improve the quality of reconstructed images. Therefore, we introduce a nonlocal similarity regularization term into the SR model shown in Eq. (2) to enhance the visual effect of the image. For each local patch $\hat{\mathbf{x}}_i$ in the reconstruction HR image $\hat{\mathbf{X}}$, it can be estimated by the weighted average of its similar patches $\hat{\mathbf{x}}_i^j$ which is found in a sufficiently large area around $\hat{\mathbf{x}}_i$. Let χ_i be the central pixel of patch $\hat{\mathbf{x}}_i$, and

χ_i^j be the central pixel of patch \mathbf{x}_i^j , and $\hat{\chi}_i$ be the estimation of the center pixel of the reconstructed image patch $\hat{\mathbf{x}}_i$. Then, $\hat{\chi}_i$ can be expressed as:

$$\hat{\chi}_i \approx \sum_{j=1}^J w_i^j \chi_i^j \quad (7)$$

The conventional NLM regularization term [11] calculate the similarity weight only based on the pixel values of the patches may lead to inaccurate estimation because of the noise and significantly-changed local structures. Here, we exploit the directional information of each pixel position and Spatial location information between pixels to develop the Combined NLM(C-NLM) regularization term to enhance weight estimation. In this paper, adopting the feature extraction of the 3.1 section, we get the direction feature information of the target pixel in the 16 directions, and further optimize the estimation of the similarity weight based on the spatial location information between pixels. Therefore, the C-NLM similarity weights can be defined by

$$w_{ij} = \exp\left(-\frac{\|\mathbf{x}_i - \mathbf{x}_i^j\|_2^2}{\rho_0} - \frac{\|\chi_i(u,v) - \chi_i^j(u,v)\|_2^2}{\rho_1} - \frac{\|\mathbf{V}_{\chi_i} - \mathbf{V}_{\chi_i^j}\|_2^2}{\rho_v}\right) \quad (8)$$

where $\chi_i(u,v)$ is the two-dimensional coordinates of the center pixel χ_i in the image, \mathbf{V}_{χ_i} is the directional feature vector of the center pixel χ_i , denoted as $\mathbf{V}_{\chi_i} = [A_{1,\chi_i}, A_{2,\chi_i}, \dots, A_{16,\chi_i}]^T$ and here, A_f ($f = 1, \dots, 16$) is the directional feature image obtained by the 3.1 section. ρ_0 , ρ_1 and ρ_v are the filter parameters to control the pixel values of the image patches, the spatial coordinates of the pixels and the directional feature information, respectively. The weight matrix obtained by Eq.(8) is substituted in (7), and then we reformulate Eq.(7) as the matrix form by $\hat{\mathbf{X}} = \arg \min \left\{ \sum_{i \in X} \|\mathbf{x}_i - \mathbf{w}_i^{C-NLM} \mathbf{S}_i\|_2^2 \right\} = \arg \min \|\mathbf{I} - \mathbf{B}\|_2^2$, where \mathbf{w}_i^{C-NLM} represents the weight matrix and \mathbf{S}_i represents a column vector consisting of the k neighbors with the largest weights related to x_i ,

\mathbf{I} is the identity matrix and $\mathbf{B}(i, j) = \begin{cases} \mathbf{w}_{ij}^{C-NLM}, & j \in \mathbf{S}_i \\ 0, & j \notin \mathbf{S}_i \end{cases}$.

In this way, we can write the non-local self similarity constraints term as:

$$E_{nonlocal}(\mathbf{X}) = \|\mathbf{I} - \mathbf{W}\|_2^2 \quad (9)$$

3.3 Steering Kernel Regression Regularization Term

The C-NLM regularization term exploits the non-local redundant information in the natural images. As a complementary regularization term to C-NLM, we further introduce the local prior information into the SR model shown in Eq. (2) to obtain a more robust super-resolution reconstruction. The pixels in the reconstruction HR image can be predicted from a small neighborhood area, i.e.,

$$\hat{\mathbf{x}}_i = \arg \min_{\mathbf{x}_i} \sum_{j \in N(x_i)} (\mathbf{x}_j - \mathbf{x}_i)^2 \mathbf{w}_{ij} \quad (10)$$

Where $\mathcal{N}(x_i)$ stands for the neighbors of x_i , w_{ij}^k is the controllable kernel which assigns larger weights to nearby similar pixel while smaller ones to farther non-similar pixels. In this paper, we employ the steering kernel proposed in [12] to calculate the weights. Putting it into eq.(10), then the formulate can be rewritten in matrix form: $\bar{\mathbf{X}} = \arg \min \left\{ \sum_{i \in \mathcal{X}} \|\mathbf{x}_i - \mathbf{w}_i^{\text{SKR}} \mathbf{L}_i\|_2^2 \right\} = \arg \min \|\mathbf{I} - \mathbf{P}\mathbf{X}\|_2^2$. where $\mathbf{w}_i^{\text{SKR}}$ represents the weight matrix and \mathbf{L}_i represents a column vector consisting of neighborhood pixels centered at x_i , \mathbf{I} is

the identity matrix and $\mathbf{P}(i, j) = \begin{cases} \mathbf{c}_{ij}^{\text{SKR}}, & j \in \mathbf{L}_i \\ 0, & j \notin \mathbf{L}_i \end{cases}$.

In such a way, we form the local prior regularization term as:

$$E_{\text{local}}(\mathbf{X}) = \|\mathbf{I} - \mathbf{P}\mathbf{X}\|_2^2 \quad (11)$$

Optimization of the algorithm

By incorporating both the sparse hallucination regularization term obtained in Eq.(6), the nonlocal C-NLM regularization term from Eq.(9) and the local prior regularization term gained in Eq.(11) into the unified reconstruction framework in Eq.(3), we have the energy function as follows:

$$E(\mathbf{X}) = \|\mathbf{Y} - \mathbf{S}\mathbf{H}\mathbf{X}\|_2^2 + \lambda_1 \|\mathbf{X} - \mathbf{Z}\|_2^2 + \lambda_2 \|\mathbf{I} - \mathbf{W}\mathbf{X}\|_2^2 + \lambda_3 \|\mathbf{I} - \mathbf{P}\mathbf{X}\|_2^2 \quad (12)$$

In this paper, we employ the gradient descent method to optimize the solution: $\bar{\mathbf{X}}^{(t+1)} = \bar{\mathbf{X}}^{(t)} - \tau \nabla E(\mathbf{X})$. where t is iteration times and τ is the step size. The gradient of the energy function is written as

$$E(\mathbf{X}) = (\mathbf{Y} - \mathbf{S}\mathbf{H}\mathbf{X})(\mathbf{S}^T \mathbf{S})^{-1} (\mathbf{H}^T \mathbf{H})^{-1} + \lambda_1 (\mathbf{X} - \mathbf{Z}) + \lambda_2 (\mathbf{I} - \mathbf{W})^T (\mathbf{I} - \mathbf{W}) \mathbf{X} + \lambda_3 (\mathbf{I} - \mathbf{P})^T (\mathbf{I} - \mathbf{P}) \mathbf{X} \quad (13)$$

Experimental results

In order to validate the effectiveness of the proposed SR method, we conduct super-resolution reconstruction experiments on a variety of natural images. In our implementation, the magnification factor is 3, the image training set is derived from the natural images applied by the Zeyde's algorithm, the dictionary size is selected as 256, and the training dataset are partitioned into 16 clusters. In the non-local constraints, the filter parameters ρ_0 , ρ_1 and ρ_v are set to 50, 40, and 30, respectively. In addition, the step size τ is set to 2.5 in the iterative process. The regularization parameters in the model are set to 0.03, 2.3 and 0.6, respectively through experimental adjustment. We compare our method with three representative methods, including SISR [5] and ASDS [7], and the Bicubic interpolation. In order to comprehensively evaluate the performance of compared SR approaches, we apply both objective and subjective assessments in experiments.

To demonstrate the visual quality of the various methods, the SR results with a magnification factor of 3 on the **Girl**, **Butterfly** and **Foreman** images are presented in Fig.1, 2 and 3, respectively. The region of interest (ROI) in each resultant image is magnified by Bicubic interpolation with factor of 2 and shown in the corners to

illustrate the high-frequency details in different images. From the visual comparison results, we notice that the Bicubic interpolation algorithm tends to produce over-smoothness and noticeable ringing artifacts along edges. Compared with the Bicubic interpolation, SISR and ASDS method can generate more clear details, but there are still many noticeable zigzagging effects found along edge. The proposed method that incorporates additional information of the LR itself and the image database produce sharper edges and pleasing details. As shown in the local magnification of ROIS in Fig.6, we can clearly see the texture of the butterfly in the resultant image of our method, while other algorithms are fuzzy.

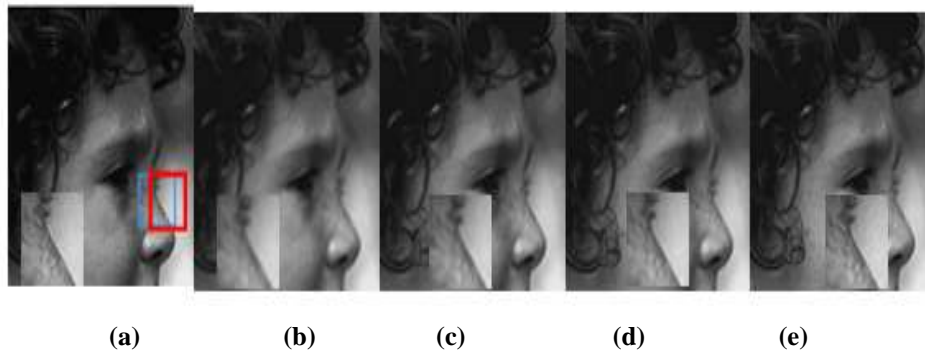


Fig.1 Comparison of SR results(3x magnification) Girl image. The local magnification of ROI in (a) is presented in the bottom-left corner of each resultant image. (a) Original HR image. (b) The Bicubic interpolation. (c) SISR. (d) ASDS (e) The Proposed method.

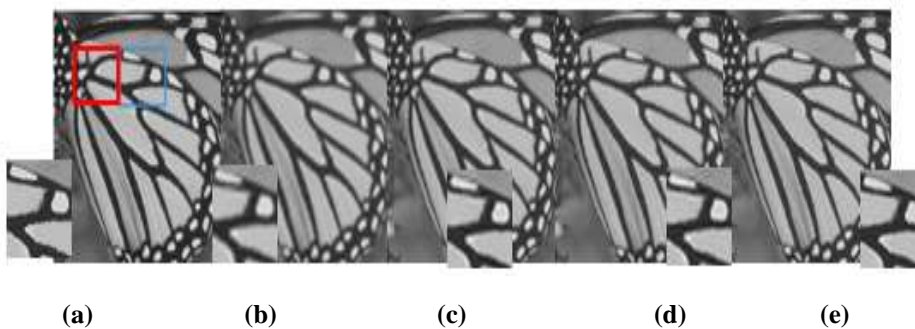


Fig.2 Comparison of SR results(3x magnification) Butterfly image. The local magnification of ROI in (a) is presented in the bottom-left corner of each resultant image. (a) Original HR image. (b) The Bicubic interpolation. (c) SISR. (d) ASDS (e) The Proposed method.

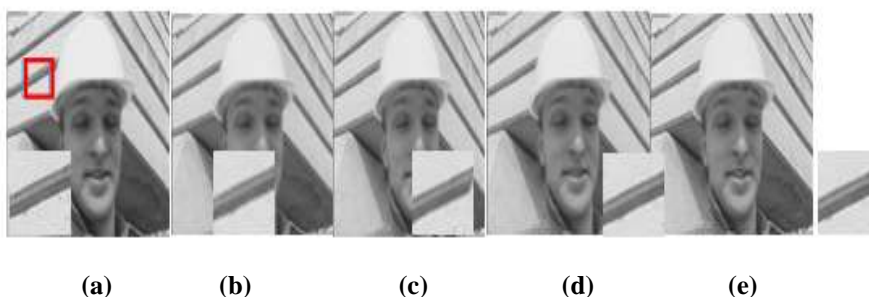


Fig.3 Comparison of SR results(3x magnification) Foreman image. The local magnification of ROI in (a) is presented in the bottom-left corner of each resultant image. (a) Original HR image. (b) The Bicubic

interpolation. (c) SISR. (d) ASDS (e) The Proposed method

Objectively, we evaluate the quality of the resultant images with via Peak Signal to Noise Ratio(PSNR) and Structural Similarity (SSIM)metrics[13].Table 1 reports the PSNR and SSIM results of the above four algorithms with x3 magnification factors when applied to the ten test images. As presented in Table1, our method is superior to the other SR approaches in terms of average metric values. The average metric values of the Bicubic interpolation algorithm is the lowest, because it only considers the smoothness prior of the image. Taking into account the sparse prior, local and nonlocal information of the image, the PSNR/SSIM results has greater improvement than the Bicubic interpolation.In addition, this algorithm exploit the test image itself to guide the multi-dictionary learning is able to provide high-res images with best recover accuracy and the Combined NLM(C-NLM) regularization term constructed can further improve the expression accuracy of image patches, thus the reconstruction effect relative to the other three algorithms have certain improvement.

Table 1

PSNR(dB)and SSIM results(3x) on ten test images. For each test image, there are two rows. The first row is the PSNR and the second one is the SSIM.

NO.	Image	Bicubic	SISR[5]	ASDS[7]	Proposed
a	Peppers	31.20	33.02	33.26	33.43
		0.9513	0.9604	0.9728	0.9746
b	Parthenon	26.03	26.67	26.92	27.21
		0.7824	0.8091	0.8213	0.8307
c	Plants	30.02	32.56	32.87	33.05
		0.8621	0.8993	0.9102	0.9186
d	Ship	29.26	30.24	30.46	30.78
		0.8522	0.8647	0.8681	0.8793
e	Parrots	27.01	28.69	29.03	29.36
		0.8018	0.8192	0.8237	0.8361
f	Hat	28.85	30.41	30.35	30.66
		0.8324	0.8467	0.8439	0.8540
g	Girl	31.14	33.35	33.60	33.93
		0.7881	0.8162	0.8247	0.8355
h	Foreman	32.94	34.43	33.84	34.17
		0.8893	0.9116	0.9198	0.9304
i	Lena	30.09	32.67	32.98	33.20
		0.9023	0.9182	0.9238	0.9287
j	Butterfly	23.17	26.18	26.31	26.72
		0.8293	0.8792	0.8903	0.9094
Avg. PSNR		28.97	30.82	30.96	31.25
Avg. SSIM		0.8491	0.8725	0.8799	0.8897

II. CONCLUSION

In this paper, we proposed a novel multi-dictionaries learning based upon directional feature classification for single image SR to solve the classification dictionary learning problem. The method exploit extra information from both the low resolution image itself and the image database.By extracting the features of the low resolution image as a priori information, the image patches satisfying a certain condition in the database are classified with the supervision of the priori information, and then use the PCA method to learn the compact classification dictionary.In the process of reconstruction, the proposed method employs the geometric information to optimize the non-local regularization technique and incorporates the complementary local steering kernel regression regularization term into the reconstruction-based SR framework to maintain sharp edges and recover more high-frequency details. It is experimentally shown that the proposed method can improve the quality of the reconstructed image and provide more details.

REFERENCES

- [1]. KIM Kwang In, KWON Younghee. Single-image super-resolution using sparse regression and natural image prior [J]. *Pattern Analysis & Machine Intelligence IEEE Transactions on*, 2010, 32(6): 1127-33.
- [2]. TIMOFTE Radu, DE Vincent, GOOL Luc Van. Anchored Neighborhood Regression for Fast Example-Based Super-Resolution; proceedings of the IEEE International Conference on Computer Vision, F, 2013 [C].
- [3]. YANG Jian-chao , Wright John , Huang Thomas, et al. Image super-resolution as sparse representation of raw image patches [C].*Computer Vision and Pattern Recognition(CVPR) 2008. IEEE Conference on*, 2008, pp. 1-8.
- [4]. YANG Jian-chao , Wright John , Huang Thomas, et al. Image Super-Resolution Via Sparse Representation [J]. *IEEE Transactions on Image Processing A Publication of the IEEE Signal Processing Society*, 2010, vol. 19, pp. 2861-2873
- [5]. ZEYDE Roman , ELAD Michael , PROTTER Matan. On single image scale-up using sparse-representations.[C] *International Conference on Curves and Surfaces*, 2010, pp:711-730
- [6]. YIN Hai-tao , LI Shu-tao ,HU Jian-wen. Single image super resolution via texture constrained sparse representation [J]. 2011, 1161-4.
- [7]. DONG Wei-sheng , ZHANG Lei , SHI Guang-ming , et al. Image deblurring and super-resolution by adaptive sparse domain selection and adaptive regularization [J]. *IEEE Transactions on Image Processing A Publication of the IEEE Signal Processing Society*, 2011, 20(7): 1838-57.
- [8]. EMMANUEL J C, DONOHO D L. Curvelets - A Surprisingly Effective Nonadaptive Representation For Objects with Edges [J]. *Astronomy & Astrophysics*, 2000, 283(3): 1051-7.
- [9]. A. M. Bruckstein, D. L. Donoho, and M. Elad. From sparse solutions of systems of equation to sparse modeling of signals and images. *SIAM Rev.* vol. 51, no. 1, pp. 34-81, Feb. 2009
- [10]. ELAD M, AHARON M. Image denoising via sparse and redundant representations over learned dictionaries [J]. *IEEE Transactions on Image Processing*, 2006, 15(12): 3736-45.
- [11]. PROTTER M, ELAD M, TAKEDA H, et al. Generalizing the Nonlocal-means to super-resolution reconstruction [J]. *IEEE Transactions on Image Processing A Publication of the IEEE Signal Processing Society*, 2009, 18(1): 36-51.
- [12]. TAKEDA H, FARSIU S, MILANFAR P. Kernel Regression for Image Processing and Reconstruction [J]. *Image Processing IEEE Transactions on*, 2007, 16(2): 349-6
- [13]. X. Gao, W. Lu, D. Tao et al. Image quality assessment based on multiscale geometric analysis[J]. *IEEE Trans. Image Process.* ,Vol. 18, no. 7, pp. 1409-1423, Jul. 2009.